Level structure of ^{101}Tc investigated by means of massive transfer reactions

H. Dejbakhsh, G. Mouchaty, and R. P. Schmitt
Cyclotron Institute, Texas A&M University, College Station, Texas 77843
(Received 2 November 1990)

The structure of ^{101}Tc has been studied using the ^{100}Mo(^{7}Li,$\alpha 2n$) reaction at 49 MeV. Both particle-γ and particle-γ-γ coincidence experiments were performed. The intensities of γ rays both in and out of the reaction plane were measured to obtain information on the ΔI of the transitions. A new band based on the $\pi g_{9/2}$ configuration was identified for the first time. To investigate the shape coexistence or configuration dependent deformation in this nucleus, interacting-boson-fermion-model and cranked shell-model calculations have been performed. Cranked shell-model calculations were used to interpret the states at higher excitation energies.

I. INTRODUCTION

It has long been known that in reactions of heavy ions lighter than Ar an abundance of light ($Z=1,2$) particles are produced with energies much higher than those from evaporation [1]. In these massive-transfer (MT), or incomplete fusion, reactions a light energetic fragment from the projectile is emitted in the field of the target, while the remaining part of the projectile fuses with the target. The resulting system formed from the massive fragment plus the target deexcites like a compound nucleus by evaporation of particles and by γ-ray decay. The light fragment from the projectile (typically a proton or an α particle) is observed as a forward energetic particle.

In the past few years, it was shown that the MT reaction is a very useful technique [2] for studying the nuclear structure of neutron-rich nuclei, which are difficult to study by more conventional heavy-ion reactions. The potential application of the incomplete fusion (or MT) reactions to nuclear structure, especially high-spin studies, was first recognized by Inamura *et al.* [3]. Theoretical calculations that attempt to describe this reaction mechanism generally assume localization in l space. The heavier the transferred fragment, the more orbital angular momentum is transferred. A recent investigation of the γ-ray multiplicity distributions associated with the MT reactions supports the picture of an l window associated with massive-transfer reactions [3]. This characteristic is very useful for studying the high-spin states of neutron-rich nuclei. In general, the advantages of the MT reaction relative to the (HI,xn) reactions in nuclear structure studies are as follows: (a) the selective population of high-spin states (difference in yrast feeding patterns); (b) the population of distinctively different mass regions than fusion reactions; (c) exit channel selectivity obtained by gating on the fragment energies (due to the correlation between the deposited excitation energy and the kinetic energy of the outgoing fragment).

The neutron-rich nuclei in the mass-100 region have been studied extensively in recent years. One of the main reasons is the nature of the shape transition, which displays a complex low-lying structure. The coexistence and competition between various forces acting inside these nuclei is responsible for this complex structure. The existence of two subshell closures, $Z=38$ or 40 and $N=56$, as well as the disappearance of these energy gaps for specific nucleonic numbers contribute to the complexity of the low-lying structures. In particular, transitional nuclei with numbers of active nucleons intermediate between the two limits, spherical and strongly deformed, are more difficult to describe. In transitional nuclei the shell force, or restoring force of the quasiparticle vacuum (collective core), is comparable to or smaller than the quasiparticle forces. Therefore, the shapes of the transitional nuclei in this region may respond to the driving force of the excited quasiparticles due to the softness of the core. The high-spin behavior of these nuclei is in general strongly influenced by the alignment along the axis of rotation of an individual nucleon in a specific orbital. The shape polarization of the nucleus is ultimately related to this effect and provides a straightforward link between the individual alignments and the shape changes in the whole nucleus. We investigated the rotational alignment with particular emphasis on the backbending aspects of the odd-A nuclei.

In the present study we have used the ^{100}Mo(^{7}Li,(p, d, t or α)$xn\gamma$) reaction. Although the massive-transfer experiment provides information on many nuclei, we only discuss one of the specific exit channels, namely, ^{100}Mo(^{7}Li,$\alpha 2n\gamma$)^{101}Tc, but will give a general overview of the whole experiment. Low-spin states associated with the negative-parity band have been studied by β decay [4] of Mo and by particle spectroscopy using the ^{100}Mo(^{3}He,d) reaction [5]. When the current study was first started, nothing was known about the $\pi g_{9/2}$ configuration except the fact that $\frac{9}{2}^+$ is the ground state in ^{101}Tc and that the $\frac{7}{2}^+$ and $\frac{5}{2}^+$ states lie at 9 and 15 keV, respectively. In this work the band associated with the $\pi g_{9/2}$ configuration up to $\frac{21}{2}^+$ was observed for the first time. This band shows a large signature splitting, which has been associated with a large γ deformation for some of the nuclei (e.g., Ag) in this region [6]. The $Z=40$ is an active subshell closure [7] for nuclei with

$38 < Z < 44$ and $N < 60$; therefore, the shape transition for the Tc isotopes is different from those with a nonactive subshell closure ($Z > 45$, e.g., Ag). This region is known to have very abrupt shape transitions, with a few nucleons making the difference between a spherical and a deformed character. This shows an important interplay between collective and single-particle forces, where in a very localized mass region, the dominant degree of freedom changes back and forth. The importance of neutron-proton interactions in the structure of the nuclei in this region has also been demonstrated previously [8]. In what follows we will discuss these various effects and describe the high-spin states using cranked shell-model calculations.

II. EXPERIMENTAL PROCEDURES

As mentioned earlier a major advantage of the MT reaction to (HI,xn) reaction is the selective population of the high-spin states. To illustrate this point a comparison of experimental results from (HI,xn) and MT reactions for positive- and negative-parity states in both the one- and the three-quasiparticle bands in ^{103}Rh are shown in Fig. 1. The ^{103}Rh data were obtained using standard in-beam spectroscopy techniques by bombarding a ^{100}Mo (2-mg/cm^2) target with a 7-MeV/nucleon ^{7}Li beam. The results for the MT reaction were obtained by bombarding a ^{100}Mo target (2 mg/cm^2) with a 6-MeV/nucleon ^{11}B beam. Selecting a specific energy window of the α particle optimizes the ^{103}Rh production from the (α,4n) channel. The gamma-ray intensities in both reactions were normalized using a specific transition. The results show a large difference between $\pi p_{1/2}$ and $\pi g_{9/2}$ both for one- and three-quasiparticle bands. The enhancement of the one-quasiparticle $\pi g_{9/2}$ band is much larger than that of the $\pi p_{1/2}$ band. There is a factor-of-two enhancement for high-spin states (three-quasiparticle band) of the high-J orbital ($\pi g_{9/2}$) in the MT reaction relative to the (HI,xn) reaction. The enhancement factor is smaller for high-spin states (three-quasiparticle band) of the low-J ($\pi p_{1/2}$) orbital. This figure clearly shows the advantage of the MT reaction in studying high-spin states. Further, the large cross section for this reaction makes a structure study feasible. We used the massive-transfer (MT) reaction technique to study neutron-rich nuclei in the mass-100 region, most of which are adjacent to a deformed region.

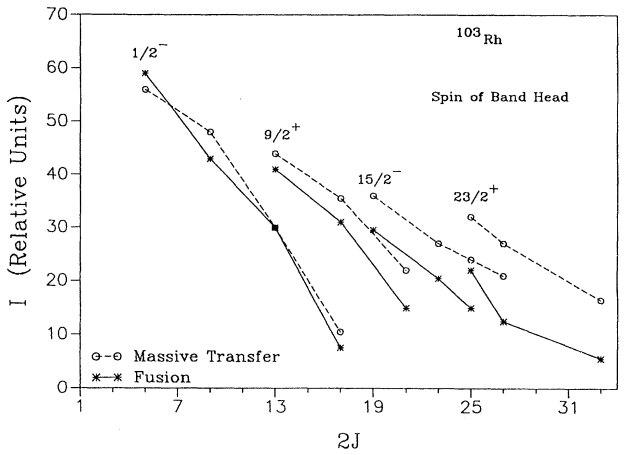

FIG. 1. Comparison of relative intensity of one- and three-quasiparticle states for both negative- and positive-parity bands in ^{103}Rh. The data were obtained through in-beam spectroscopy measurements on the ^{100}Mo(^{7}Li,4n)^{103}Rh reaction at 49 MeV and the massive-transfer reaction ^{100}Mo(^{11}B,α4n)^{103}Rh at 62 MeV.

The MT technique enabled us to investigate all nuclei associated with $Z=1$ and 2 exit channels ($^{101-104}$Ru and $^{101-103}$Tc) to much higher angular momenta than would have been possible otherwise. The data were obtained using particle γ-ray spectroscopy based on the massive-transfer reactions. An enriched self-supporting metallic target of ^{100}Mo with 2$\sim$mg/cm^2 in thickness was bombarded with a 49-MeV ^{7}Li beam from the Texas A&M University Cyclotron. The energetic light particles at 20° were detected with Si telescopes located about 7 cm from the target. The aperture of the particle detectors had about 1 cm^2 opening, giving an angular definition of about ±4°. Thin Al foils were placed over the apertures to prevent elastically beam particles from reaching the detectors.

The results of three separate experiments are reported here. The first experiment used one particle stack, while the second and third experiments employed three sets of particle stacks, two in the horizontal plane containing the beam axis, at about ±20° with respect to the beam direction, and one in the perpendicular plane at 20°. Since detecting a particle defines a reaction plane and thus a spin direction (on average perpendicular to this plane), this geometry yields information on the ΔI values of the γ-ray transitions. Each stack consisted of three surface-barrier Si detectors with different thicknesses (300, 1000, and 5000 μm). In the first and third experiments two Ge(Li) detectors were placed at ±90° with respect to the beam axis. In the second experiment three Ge(Li) detectors were positioned at +90°, 120°, and 150° relative to the beam direction. Most of the data (>55%) reported here were collected in the last experiment.

Coincidences were demanded between particles in the Si telescopes and γ rays in any Ge(Li) counter. Since the rate for the particle-γ-γ coincidences was at least 10 times lower than that for particle-γ coincidences, only a small fraction of the collected data actually gave particle-γ-γ information. Both types of data were recorded on an event-by-event basis on magnetic tape. For each particle type, γ-γ coincidence matrices were constructed and gain shifted to a common gain. The data from all three experiments were summed in order to achieve the maximum statistics possible for the γ-γ matrix.

The level structure reported here is based on particle-γ-γ coincidence data extracted from the raw data. About 4.5×10^6 particle-γ-γ coincidence events were collected through all three experiments. These events were spread over at least seven different exit chan-

nels ($^{101-104}$Ru and $^{101-103}$Tc); the highest statistics belonged to ^{102}Ru for $Z=1$ and ^{101}Tc for $Z=2$ particles. The total number of particle-γ-γ coincidences for the ^{100}Mo(^{7}Li,$\alpha 2n$)^{101}Tc reaction channel was greater than 0.5×10^{6}. This might not seem to be adequate statistics, but one should keep in mind that the spectrum for each exit channel of an MT reaction is very clean relative to the spectrum from a conventional heavy-ion fusion reaction. Figures 2(a) and 2(b) illustrate the differences between the two cases. The former shows the total γ-ray spectrum for reactions of 49-MeV ^{7}Li with a ^{100}Mo target while the latter shows the γ-ray spectrum for the same reaction in coincidence with α particles in a specific energy window. The appropriate energy gate for the particles

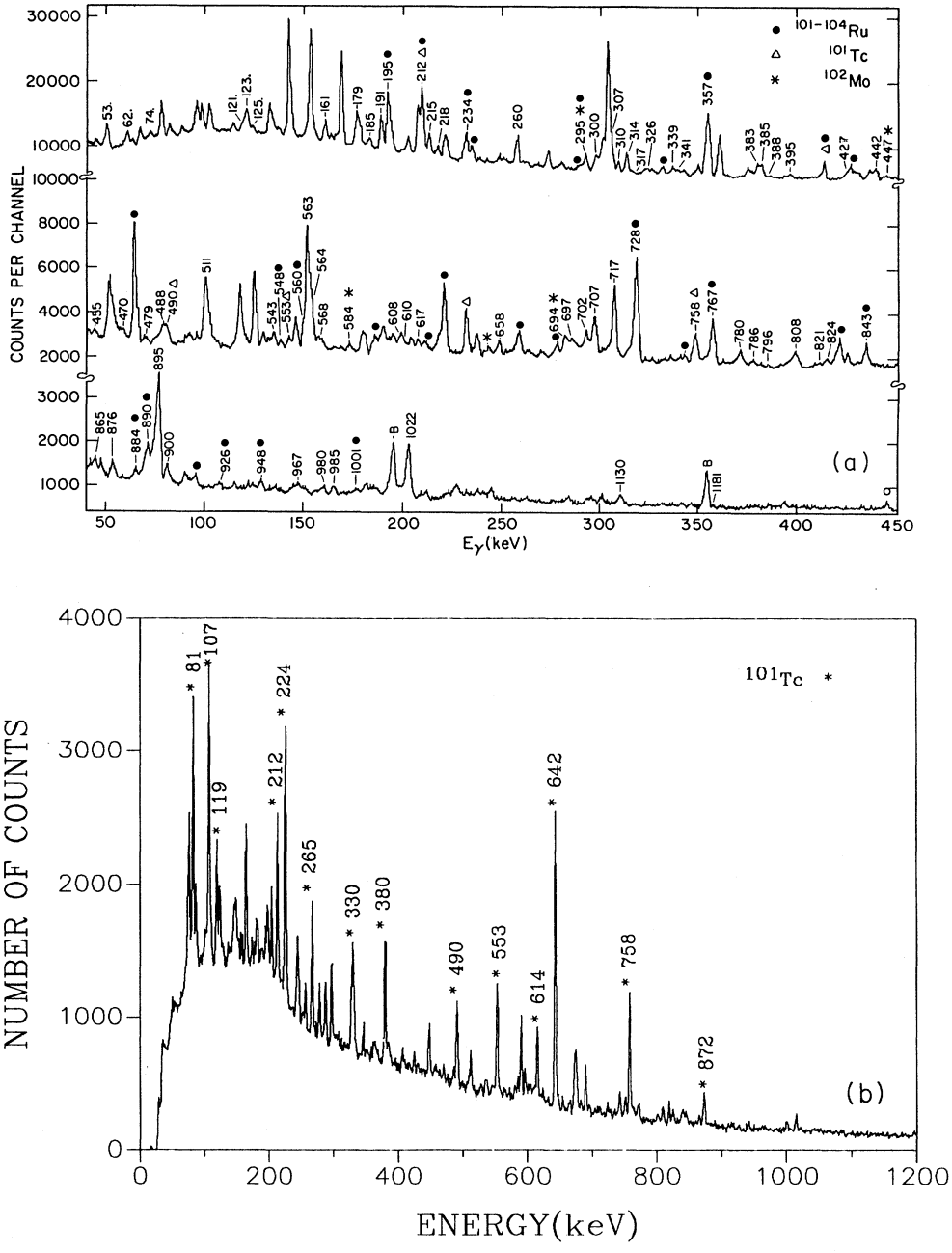

FIG. 2. (a) Gamma-ray spectrum from the bombardment of ^{100}Mo with a 49-MeV ^{7}Li beam. (b) Total gamma-ray spectrum for massive-transfer reaction channels for the same reaction as part (a). The spectrum was obtained by gating on α particles in a specific energy window.

was determined by investigating the energy spectra of practicles in coincidence with discrete transitions. The energy range of the α particles was chosen to be 35–52 MeV (in the laboratory system) to optimize the ^{101}Tc production.

Information on γ-ray multipolarities and intensities (I_γ) was obtained from in-plane and out-of-plane measurements. The anisotropy information was used to make spin assignments, assuming a high degree of alignment of the high-spin states of the residual nuclei, and their subsequent decay by stretched $E2$ transitions, for the yrast states. These assumptions have been found to be reasonably good for massive-transverse reactions [2]. This approach provides the change in the angular momentum, ΔI, for the transitions, but does not give either the sign of ΔI or the parity change. However, by invoking the yrast argument ($I_i = I_f + \Delta I$), some of the ambiguities could be resolved.

III. EXPERIMENTAL RESULTS

The level structure of ^{101}Tc deduced from the present work is shown in Fig. 3. The energies, relative intensities, and the in-plane/out-of-plane anisotropies of γ rays observed for the ^{100}Mo(^{7}Li,$\alpha 2n$)^{101}Tc reaction at 49 MeV are presented in Table I. The first column lists the γ-ray energies for more than 20 γ-ray transitions assigned to ^{101}Tc. The relative intensities at 90° with respect to the beam direction in coincidence with the in-plane particle detectors stacks are given in the second column. The in-plane/out-of-plane ratios are shown in the third column. The placements of the transitions are listed in the fourth column. The level scheme was constructed primarily from coincidence relationships. The order of the transitions was determined from the intensities in the coincidence spectra. While the transition energies were used to confirm placement, no γ ray was placed in the level scheme solely on the basis of its energy. Each band in the level scheme will be discussed separately.

A few $\Delta I = 1$ transitions from the negative-parity band based on the $\frac{1}{2}^-$ state were known previously from decay studies [5]. The extension of this band up to 2.2 MeV of excitation energy is firmly established by coincidence relationships with known transitions [see Fig. 4(a)]. The spin of $\frac{1}{2}^-$, $\frac{3}{2}^-$, and $\frac{5}{2}^-$ were assigned to the 207-, 288-, and 395-keV levels in previous studies [5]. The values of the in-plane/out-of-plane ratios in this work support these assignments. The in-plane/out-of-plane ratio of the 119-keV transition leads to a spin assignment of $\frac{7}{2}^-$ for the 619-keV level. On the basis of in-plane/out-of-plane data, spin assignments of $\frac{11}{2}^-$ and $\frac{15}{2}^-$, were made for the 947- and 1500-keV levels, respectively. A strong stretched $E2$ cascade was observed in coincidence with 380-keV transitions which deexcites the $\frac{5}{2}^-$ to $\frac{5}{2}^+$ states. Based on the in-plane/out-of-plane ratio of the 489- and 614-keV γ transitions, spin assignments of $\frac{9}{2}^-$ and $\frac{13}{2}^-$ were made for the 884- and 1498-keV levels. All the

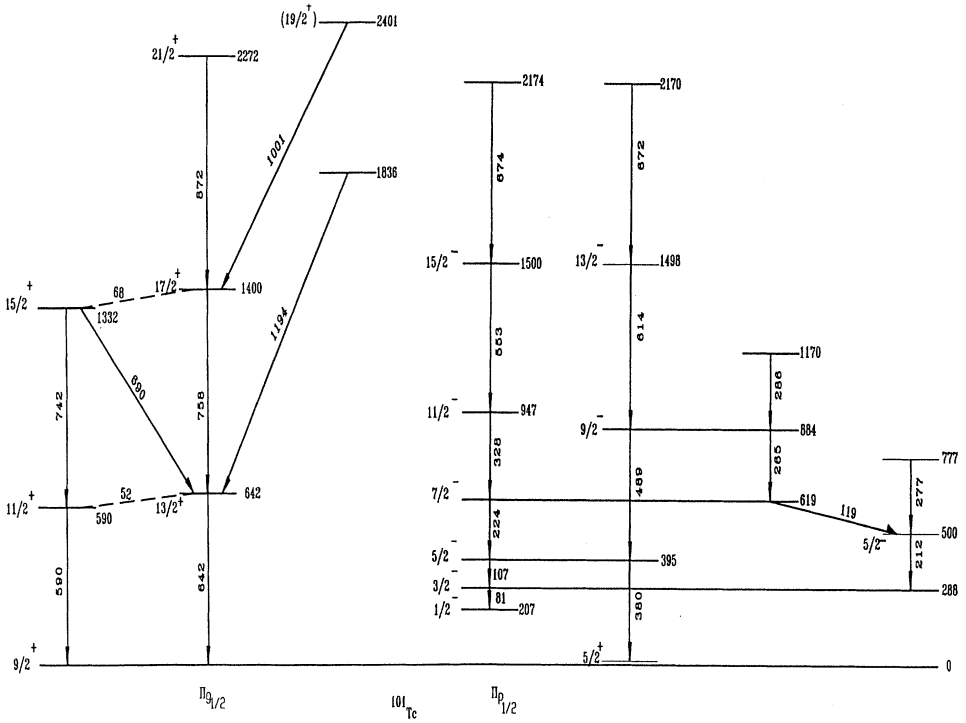

FIG. 3. Level structure of ^{101}Tc obtained from the reaction ^{100}Mo(^{7}Li,$\alpha 2n$)^{101}Tc at 7 MeV/nucleon.

transitions and the levels above $\frac{5}{2}^-$ (395 keV) in this negative-parity band are new and have not been reported previously.

A strong stretched $E2$ cascade based on the $\frac{9}{2}^+$ ground state was observed for the first time. A coincidence spectrum for this positive-parity band is shown in Fig. 4(b). The quadrupole nature of the 642-, 758-, and 872-keV γ transitions established from the in-plane/out-of-plane ratios, yielding spin assignments of $\frac{13}{2}^+$, $\frac{17}{2}^+$, and $\frac{21}{2}^+$ for the 642-, 1400-, and 2272-keV levels, respectively. We reported this band previously in connection with the blocking experiment in the $A=100$ region [9].

IV. DISCUSSION

The level structure of ^{101}Tc will be discussed within the framework of two different theories. The low-lying collective band based on one-quasiproton configurations will be investigated using the interaction boson-fermion model (IBFM) [10,11]. Band crossing and signature splitting for this nucleus will be discussed based on the cranked shell-model (CSM) calculations [12].

A. IBFM description

Several theoretical studies [13,14] have been devoted to the interpretation of the experimental results of β-decay [15] and particle-transfer reactions [16,17] forming Tc isotopes. In the IBFM analysis of available data on $^{97-103}$Tc by De Gelder *et al.* [18] considerable deviation was found between experimental and calculated low-lying levels of ^{101}Tc. De Gelder *et al.* considered Ru isotopes as cores in their investigation.

Since the calculation of De Gelder *et al.* of the odd-Z Tc nuclei included only three low-lying levels in ^{101}Tc, we

TABLE I. The γ-ray energies, intensities, and in-plane/out-of-plane anisotropies measured for the $^{100}(^7\text{Li},\alpha 2n)^{101}$Tc reaction at 49 MeV. α particles were observed at 20° with respect to the beam direction.

Energy[a] (keV)	I_γ(rel)[a]	In-plane/Out-of-plane anisotropy	Placement
80.9	25.21	0.797 (26)	288→207
107.4	18.28	0.527 (19)	395→288
118.9	5.18	0.766 (53)	619→500
212.0	15.39	0.883 (35)	500→288
224.1	25.22		619→395
265.8	13.56		884→619
277.5	6.45		777→500
286.3	6.04		1170→884
295.4	15.05	1.359 (141)	
328.2	23.04	1.528 (75)	947→619
330.1	6.19		619→288
379.3	22.07	1.286 (62)	395→15
446.2	10.27	1.533 (140)	
489.6	15.27	1.476 (100)	884→395
553.2	21.51	1.484 (81)	1500→947
584.1	5.63	2.314 (566)	
589.8	31.01	1.706 (77)	590→0
591.3	8.11		
614.1	13.16	1.771 (168)	1498→884
642.3	100.00	1.657 (31)	642→0
653.1	1.71		
672.3	9.14		2170→1498
673.8	14.80		2174→1500
690.2	15.77	1.210 (77)	1332→642
694.5	5.45		
742.1	10.1	1.515 (173)	1332→590
757.8	49.86	1.607 (52)	1400→642
769.0	3.76		
771.1	6.53	1.266 (157)	
818.4	9.01	0.431 (33)	
824.6	7.06	1.453 (198)	
871.7	13.07	1.373 (124)	2272→1400
1001.1	4.63	0.856 (166)	2401→1400
1194.3	1.90	0.638 (304)	1836→642

[a] The uncertainties in the energies (intensities) are 0.3 keV (10%) for strong transitions ($I_\gamma > 20$) and 0.5 keV (20%) for the weaker transitions. The uncertainties in intensities are larger than 20% for the closely spaced doublet transitions.

decided to repeat the calculation with the same parameters for comparison with the levels at higher excitation energies. A description of the IBFM model and the parameters are given in Ref. [18]. The results of this calculation are compared with the high-lying levels of the $\pi g_{9/2}$ configuration in Fig. 5. The overall agreement between the calculation and experimental energy levels is poor, indicating the need to investigate this nucleus in the IBFM framework using a different approach. From the above results we also concluded that the shape transition

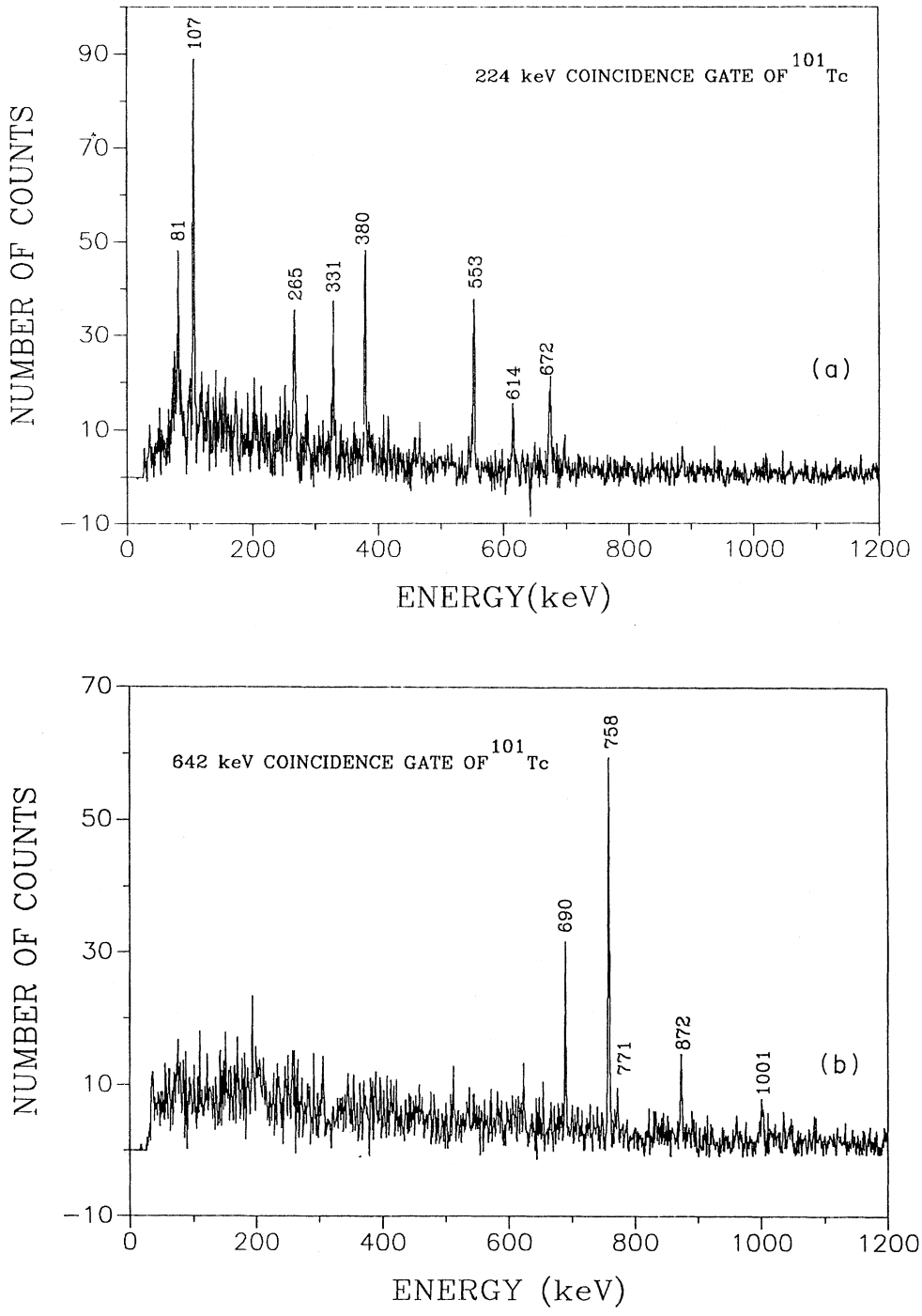

FIG. 4. (a) Coincidence spectrum gated by the 224-keV transition of the negative-parity band. (b) Coincidence spectrum of positive-parity transitions gated by the 642-keV γ ray. Both spectra have been corrected for background contributions.

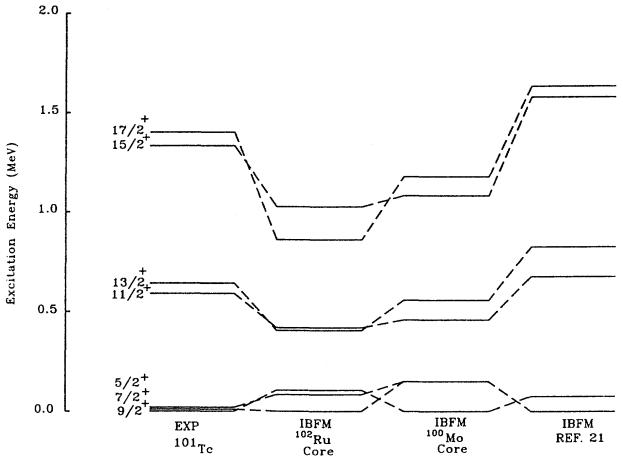

FIG. 5. Comparison of the experimental energy levels with the predictions of the IBFM model for the $\pi g_{9/2}$ band in ^{101}Tc. The parameters used in the first calculation are the same as those in Ref. [18] (see text for details).

of ^{101}Tc might be different from that of ^{102}Ru. The shape transition of the even-even Ru isotopes (including ^{102}Ru) is thought to be a change from an anharmonic vibrator ($N=54$) to a γ-unstable nucleus ($N=60$) [an SU(5) to O(6) transition].

We believe it is more appropriate to use ^{100}Mo as the core for the ^{101}Tc for the following reasons: (1) The energies for the $\frac{9}{2}^+$ band in ^{101}Tc are quite close to those in the collective 2^+, 4^+, and 6^+ states in ^{100}Mo. (2) For nuclei with $Z<45$ and $N<60$, $Z=40$ is still an active subshell. Therefore, the validity of $Z=40$ subshell closure should not be ignored for the Tc isotopes as it would be using a Ru core.

In our calculation even-even ^{100}Mo was chosen as the core, which is coupled to a fermion in a shell-model orbital of spin j. The parameters for the ^{100}Mo core were taken from Ref. [13], which describes the ^{100}Mo by IBFM-2 (this model treats neutron and proton bosons differently). The odd-proton occupies a $1g_{9/2}$ orbital in the case of the positive-partity band. In this work the parameters used in the boson-fermion interaction (A, Γ_0, and Λ_0) and v^2 were the same as those given in the Ref. [18]. The results of this calculation and the comparison with the experimental result are shown in Fig. 5. The calculated values are in good agreement with experimental data except for low-lying levels ($\frac{5}{2}^+$ and $\frac{7}{2}^+$).

The structure of $^{96-100}$Mo was explained by Sambataro *et al.* [13] using two different boson numbers ($N_\pi=1$ and $N_\pi=3$) simultaneously. When $Z=40$ subshell closure is an active shell, the number of proton bosons (N_π) is 1. Since $Z=40$ is a subshell closure, it is possible to excite a pair of protons above the $Z=40$ shell. If only one pair is excited from below, the number of proton bosons (N_π) is 3 (two pairs of protons and one pair of proton holes). This indicates that the possibility of configuration mixing should be explored for the Tc isotopes. Since the low-lying collective structure in odd-A nuclei is often similar to that of even-even neighboring (core) nuclei, an extension of the IBM with configuration mixing, which has been successful for Mo isotopes, may better predict the structure of odd-A Tc isotopes. The positive-parity states in ^{97}Tc and ^{99}Tc have been calculated within the IBFM model [19,20] using Mo isotopes as cores. For ^{97}Tc two separate calculations were carried out by Zell *et al.* [20]. The first calculation assumed one proton boson ($N_\pi=1$), implying that $Z=40$ is a valid subshell. The second calculation considered four proton boson holes ($N_\pi=4$) corresponding to the $Z=50$ shell. Some of the low-lying levels are explained well by the configuration with a larger boson number, favoring a breakdown of the $Z=40$ subshell closure. While these calculations do not include configuration mixing, they do support the idea of configuration mixing in Tc isotopes. Thus better agreement with experimental values might achieved with calculations similar to those given in Ref. [13]. However, since no $B(E2)$'s are known for this ^{101}Tc nucleus, it would be difficult to determine the deformation parameters.

Recently Arias *et al.* [21] studied both positive- and negative-parity configurations in odd-proton Rh and Tc isotopes, within the IBFM-2 framework. The authors used even-even Pd and Ru isotopes as the respective cores. The boson-fermion interaction parameters are given in Ref. [21]. The results from the Arias calculation are also shown in Fig. 5. This calculation predicts a $\frac{7}{2}^+$ state as ground state for ^{101}Tc instead of a $\frac{9}{2}^+$ state. Since the above calculation is the result of a systematic investigation, the authors believe that the predictions can be improved if one focused on an individual nucleus (such as ^{101}Tc). The above results indicate that ^{101}Tc cannot be described by simple IBFM-1 or IBFM-2 calculations. One needs to consider the mixing calculation in the IBFM framework using a more realistic approach.

B. High-spin state description

In this mass region the high-j $g_{9/2}$ proton and $h_{11/2}$ neutron intruder orbitals in the vicinity of the Fermi surface can give rise to alignment effects. The results from the first set of blocking experiments [9] firmly established that the alignment of a pair of $h_{11/2}$ neutrons with spin 10^+ and a rotational frequency of 0.37 MeV/$\hbar$ is responsible for the discontinuity in the rotational structure.

The ^{101}Tc nucleus has been studied using an axially symmetric cranked shell model even though the $\pi g_{9/2}$ band shows a large signature splitting. The CSM used in this investigation is based on independently rotating quasiparticles. The calculated crossing frequency of the different aligned configurations with the g band are deduced from plots of the quasiparticle energies $e(\omega)$ (in the rotating frame) versus the rotational frequency $\hbar\omega$. Figure 6 shows the energies $e(\omega)$ for quasineutrons in ^{101}Tc as a function of $\hbar\omega$. The crossing frequency is predicted to be $\hbar\omega=0.38$ MeV. In these cranked shell-model calculations the values of the Nilsson parameters of the modified oscillator potential, κ and μ, correspond

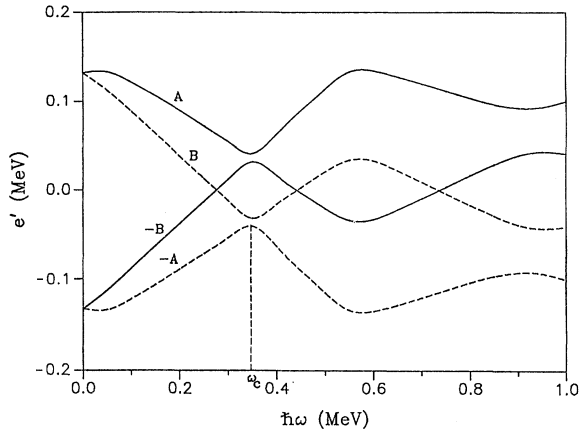

FIG. 6. Quasineutron energies for $N=58$ plotted as a function of the rotational frequency. The calculation uses $\varepsilon_2=0.17$ and $\varepsilon_4=0.0$ (other parameters are given in the text).

to the values given in Ref. [22]. The pairing strength Δ was deduced from the odd-even mass differences [23]. In the pairing correlations we included three oscillator shells, $N=2,3,4$, for the protons and $N=3,4,5$ for the neutrons. The Fermi surface energy was adjusted to give the correct number of neutrons and protons for $\omega=0$. We assumed $\varepsilon_2=0.17$ for this nucleus, based on the experimental $B(E2)$ value [24] of neighboring even-even nuclei. The hexadacapole and the γ deformations were assumed to be zero.

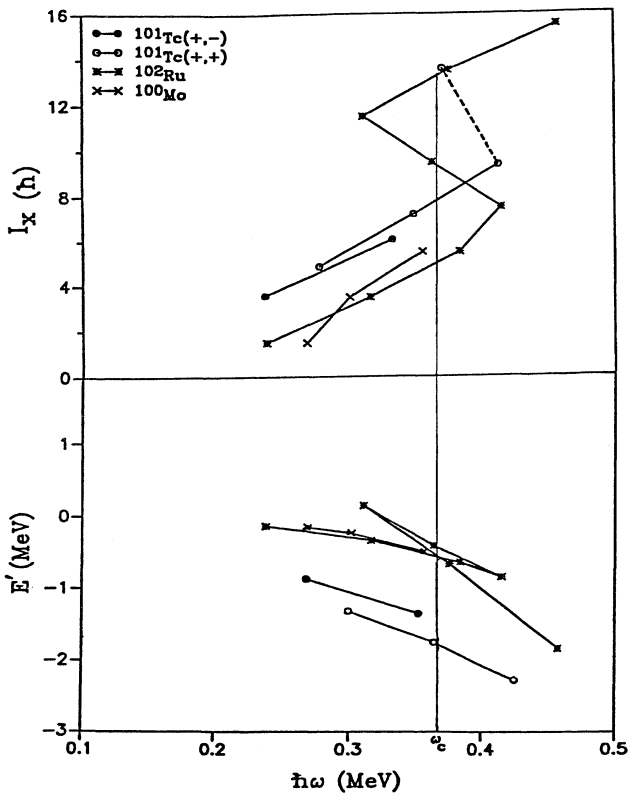

FIG. 7. Experimental Routhians and aligned angular momentum I_x as a function of rotational frequency $\hbar\omega$ for ^{101}Tc. The experimental data are from this work. The plot includes the experimental data from ^{102}Ru and ^{100}Mo for comparison.

In order to compare the rotational properties of the observed band in ^{101}Tc with the CSM calculation, we performed a cranked shell-model analysis of the experimental data. The experimental Routhian and aligned angular momentum along the rotational axis were extracted from the experimental data for comparison with the theoretical predictions for two even-even neighboring nuclei (^{102}Ru, ^{100}Mo) and ^{101}Tc. Figure 7 shows the quasiparticle Routhians, E's, and the aligned angular momenta along the rotation axis, I_x, as a function of the rotational frequency ($\hbar\omega$) for positive-parity yrast band in ^{101}Tc. This figure includes experimental values for the ground-state rotational bands in ^{100}Mo and ^{102}Ru using the prescription given in Ref. [25]. The experimental crossing frequency is shown in these plots. The CSM prediction for the crossing frequency is very close to that suggested by the experimental data. The interaction strength can be found from the CMS plot by taking half of the energy difference between the crossing trajectories, A and $-B$ in Fig. 6. The calculated interaction strength is small for even-even neighboring nucleus, ^{102}Ru, producing a sharp backbend as seen experimentally [9]. If the crossing for the $\pi g_{9/2}$ band in ^{101}Tc is similar to that in ^{102}Ru, then we predict that the next transition in ^{101}Tc will be on the order of 760 to 790 keV. We have observed a 771-keV transition in ^{101}Tc which seems to be the best candidate for the $\frac{25}{2}\rightarrow\frac{21}{2}$ transition, but the low intensity in the coincidence spectrum prevents a definite assignment. This transition has been included on the experimental aligned angular momentum for ^{101}Tc and it is shown as a dashed line in Fig. 7.

The interpretation of the $\pi p_{1/2}$ configuration (negative-parity band) is more difficult than that of $\pi g_{9/2}$ due to the mixing of the $\pi p_{1/2}$ band with other negative-parity orbitals. An interesting aspect of the negative-pairty band of the ^{101}Tc nucleus which should be explored is the fact that the strong $M1$ transitions turn to strong $E2$ transitions at low spin. This feature, which is characteristic of the shape change, has not been observed in neighboring isotopes or isotones. The authors believe that this nucleus should be investigated in the IBFM framework using the same core parameters to explain the structure of both positive- and negative-parity states.

V. CONCLUSION

We have presented experimental results on the nuclear structure of ^{101}Tc up to moderate spins. The study of this nucleus was made possible through the use of massive-transfer reactions, which have provided an unambiguous identification of the transitions in ^{101}Tc. Our investigation used charged-particle-γ and charged-particle-γ-γ coincidences and in-plane and out-of-plane anisotropy measurements to construct the level structure. More than 20 new transitions have been identified for the first

time and placed in the level structure of this nucleus.

We have studied the structure of ^{101}Tc in the framework of the interacting boson-fermion model (IBFM) using the neighboring even-even Ru and Mo isotopes as cores. The comparison of the experimental and theoretical results and previous theoretical (IBFM) calculations [18,21] sheds light on the direction of the shape transition of this nucleus.

This study suggests that the shape transition in the neutron-rich ^{101}Tc nucleus is similar to that in ^{101}Mo. We also conclude that IBFM calculations including configuration mixing will give a better description of the Tc isotopes. Because the Tc iostopes with $Z=43$ are close to the $Z=40$ subshell closure, the neutron-proton interaction strength can alter effects from the $Z=40$ subshell, leading to shape changes and shape coexistence. Shape coexistence has been observed in Mo isotopes, but has not been explored in the Tc nucleus. From the present data we conclude that the ^{101}Tc nucleus has a complex structure, requiring further theoretical investigations to explain some of the low-lying structure of this nucleus.

The high-spin data on ^{101}Tc do not extend far enough to see the backbending, but from available experimental data, a comparison with experimental results of neighboring nuclei and CSM calculations, we have tentatively concluded the following: (a) For the $\pi g_{9/2}$ band of ^{101}Tc the backbending should occur at $\frac{21}{2}^+$ with a frequency of about 0.36–0.38 MeV, due to alignment of a pair of $h_{11/2}$ neutrons. (b) The interaction strength between the two crossing bands seem to be small, indicating a sharp backbend for this nucleus.

More experimental data are needed to investigate the direction of the shape transition and explore proton-neutron interaction strength in the Tc isotopes as a function of neutron number.

ACKNOWLEDGMENTS

This work has been supported partially by the Department of Energy under Grant DE-FG05-86ER40256. One of us (R.P.S.) also acknowledges support from the Robert A. Welch Foundation under Grant A-972.

[1] H. C. Britt and A. R. Quinton, Phys. Rev. **124**, 877 (1961); J. Galin *et al.*, Phys. Rev. C **9**, 1126 (1974).
[2] T. Inamura, A. C. Kahler, D. R. Zolnowski, U. Garg, T. T. Sugihara, and M. Wakai, Phys. Rev. C **32**, 1539 (1985); H. Yamada, D. R. Zolnowski, S. E. Cala, A. C. Kahler, J. Pierce, and T. T. Sugihara, Phys. Rev. Lett. **43**, 605 (1979).
[3] T. Inamura, M. Ishihara, T. Fukuda, T. Shimoda, and H. Hiruta, Phys. Lett. **68B**, 51 (1977).
[4] J. F. Wright, W. L. Talbert, Jr., and A. F. Voigt, Phys. Rev. C **12**, 572 (1975).
[5] *Table of Isotopes,* 7th ed., edited by C. M. Lederer and V. S. Shirley (Wiley, New York, 1978).
[6] H. J. Keller, S. Frauendorf, U. Hagemann, L. Kaubler, H. Prade, and F. Stary, Nucl. Phys. **A444**, 261 (1985); S. Frauendorf, *Proceeding of International Symposium on In-Beam Nuclear Spectroscopy* (Debrecen, Hungary, 1984).
[7] R. F. Casten, Phys. Lett. **152B**, 145 (1985).
[8] H. Dejbakhsh, R. P. Schmitt, and G. Mouchaty, Phys. Rev. C **37**, 621 (1988).
[9] D. R. Haenni, H. Dejbakhsh, R. P. Schmitt, and G. Mouchaty, Phys. Rev. C **33**, 1543 (1986).
[10] F. Iachello and O. Scholten, Phys. Rev. Lett. **43**, 679 (1979).
[11] O. Scholten, Ph.D. thesis, University of Groningen, The Netherlands, 1980 (unpublished).
[12] R. Bengtsson and S. Frauendorf, Nucl. Phys. **A327**, 139 (1979).
[13] M. Sambataro and G. Molnar, Nucl. Phys. **A376**, 201 (1982).
[14] J. Stachel, P. Van Isacker, and K. Heyde, Phys. Rev. C **25**, 650 (1982).
[15] K. Summerer, N. Kaffrell, E. Stender, N. Trautmann, K. Broden, G. Skarnemajk, T. Bjornstad, and I. Haldorsen, Nucl. Phys. **A339**, 74 (1980).
[16] R. F. Casten, E. R. Flynn, Ole Hansen, and T. J. Mulligen, Nucl. Phys. **A184**, 357 (1972).
[17] E. R. Flynn, R. E. Brown, J. A. Cizewski, W. Sunier, W. P. Alford, E. Sugarbaker, and D. Ardouin, Phys. Rev. C **22**, 43 (1980).
[18] P. De Gelder, D. De Frenne, K. Heyde, N. Kaffrell, A. M. Van Den Berg, N. Blasi, M. N. Harakeh, and W. A. Sterrenburg, Nucl. Phys. **A401**, 397 (1983).
[19] D. Hippe, H. W. Schuh, U. Kaup, K. O. Zell, P. Von Brentano, and D. B. Fossan, Z. Phys. A **311**, 329 (1983).
[20] K. O. Zell, H. Harter, D. Hippe, H. W. Schuh, and P. Von Brentano, Z. Phys. A **316**, 351 (1984).
[21] J. M. Arias, C. E. Alonso, and M. Lozano, Nucl. Phys. **A466**, 295 (1987).
[22] L. E. Larsson, G. Leander, I. Ragnarson, and N. G. Alenius, Nucl. Phys. **A261**, 77 (1976).
[23] A. Bohr and M. Mottelson, *Nuclear Structure* (Benjamin, New York, 1969), Vol. I, p. 169.
[24] A. Bockisch, M. Miller, A. M. Kleinfeld, A. Gelberg, and U. Kaup, Z. Phys. A **292**, 265 (1979).
[25] R. Bengtsson and S. Frauendorf, Nucl. Phys. **A327**, 139 (1979).